ELSEVIER

Contents lists available at ScienceDirect

Polymer Degradation and Stability

journal homepage: www.journals.elsevier.com/polymer-degradation-and-stability





Artificial weathering and physico-chemical characterization of EPON-IPD thermosets with high enthalpy storage of shape memory

Tahsin Zaman ^a, Lillian T Mambiri ^b, Peyman Nikaeen ^a, Joelle A Chauhan ^b, Dilip Depan ^b, Ahmed Khattab ^a, William M Chirdon ^b, ^{*}

ARTICLE INFO

Keywords: Shape memory polymer Thermomechanical Weathering Degradation Nanoindentation DSC

ABSTRACT

While thermosetting shape memory polymers (TSMPs) hold great potential in aviation, automotive, and biomedical industries, an understanding of how they degrade under environmental conditions is needed before they can be broadly incorporated into their respective applications. This study includes a characterization of TSMP of notably high-enthalpy storage in response to artificial weathering including UV irradiation and cyclic condensation to simulate aging under terrestrial conditions. The comprehensive characterization includes differential scanning calorimetry, FTIR analysis, scanning electron microscopy with image analysis, nano-indentation, and stress and shape recovery tests after macro-scale compression. Qualitative and quantitative differences between the irradiated samples with and without condensation are observed and discussed. Glass transition temperatures increased due to crosslinking in UV-irradiated samples, while they decreased due to plasticization and hydrolysis under cyclic condensation. Similarly, UV-irradiated samples experience an increase in elastic modulus and hardness, while these properties decreased in cyclic condensation samples with exposure time. UV-irradiated samples had better stress recovery and smaller surface cracks than UV-condensation-weathered samples which had better shape recovery. The mechanisms of these fundamentally different effects are discussed.

1. Introduction

Shape memory polymers (SMPs) have stimulated considerable interest across a wide range of industries as a result of their versatility and exceptional elastic deformation properties [1]. The popularity of SMPs is attributed to their ability to change shape and recover their original shape upon external stimulation [2]. SMPs have applications in biology, energy, aeronautical engineering, civil and architectural engineering, and other fields [3,4]. High enthalpy storage in SMPs is required or desirable for many applications including self-healing materials [5]. This high enthalpy storage SMP stores energy predominantly through the enthalpy change arising from the stretched bonds during programming [5]. Also in many of these applications, such as finishing fabric, actuator and dampeners in aerospace, stents, and catheters in medical devices; SMPs are exposed to varying environmental conditions that include but are not limited to ultraviolet radiation, moisture and high temperatures. In turn, the chemical and mechanical properties of the

SMPs are significantly altered over time. Ultimately, this affects the overall performance and service life of these polymers, rendering them unsuitable for their intended applications [6,7]. Therefore, understanding the degradation mechanisms as well as the degree of degradation in shape memory functioning is critical before identifying appropriate applications and usage recommendations for these shape memory polymers (SMPs).

A number of studies have been carried out in order to determine and characterize the extent of degradation which is typically accompanied by color change as there is yellowing due to carbonyl formation from thermo-oxidation [8,9]. Water at varying temperatures significantly deteriorates the shape recoverability and morphological structure of a polyester based SMP [10–12]. One important thermo-mechanical property of SMPs that changes due to degradation is the glass transition temperature. When EPON-IPD was exposed to UV light for varied periods of time, a rise in T_g was detected. Because most polymers have bond dissociation energies in the region of UV light wavelengths,

E-mail address: wchirdon@louisiana.edu (W.M. Chirdon).

^a Department of Mechanical Engineering, University of Louisiana at Lafayette, Louisiana 70503-2007, United States

^b Department of Chemical Engineering, University of Louisiana at Lafayette, Louisiana 70503-2007, United States

^{*} Corresponding author.

exposure to the sun spectrum has a significant impact on them [13]. Absorption of ultraviolet photons by polymers causes photo-oxidative processes that results in material degradation. On the other hand, T_g decreases when SMPs are exposed to moisture due to plasticization. Moisture-induced plasticization lowers the yield stress, modulus, and strain threshold for failure [14]. UV exposure and condensation caused substantial surface deterioration, microcracks, increased roughness, and negligible changes in tensile strength in polymer-based composites [6, 12,15,16].

Previously, a study was published on the degradation of this EPON-IPD system under UV exposure with an emphasis on the chemical degradation [17]. In this paper, the effects of UV radiation are compared and contrasted to the effects of UV radiation combined with moisture cycles on the thermo-mechanical, chemical, and shape memory properties of this EPON-IPD system. UV radiation and moisture are ubiquitous in the natural environment and are thought to be the primary drivers of degradation in epoxies under ambient conditions. EPON-IPD SMPs were artificially weathered using UV irradiation alone and cyclic UV irradiation and condensation exposure for 0 h, 300 h and 600 h. Fourier transform infrared spectroscopy was used to determine chemical structure changes. And morphological changes were investigated using SEM imaging. Characterization of the thermomechanical properties was completed using nanoindentation and differential scanning calorimeter (DSC). Finally, the change in shape memory properties was pivotal to this paper therefore stress and shape recovery tests were conducted to quantify the shape memory degradation of EPON-IPD SMPs.

2. Material and methods

2.1. Materials

The thermosetting SMP was synthesized using diglycidyl ether of bisphenol A (DGEBA)-based resin (EPON 826, Miller-Stephenson Chemical Co., Inc. Danbury, CT, USA, Lot # DP21G1645/2801) and isophorone diamine hardener IPD (Sigma Aldrich, Burlington, MA, USA). Firstly, EPON was heated in an oven for 30 min at a temperature 60 °C. A mechanical mixer was used to mix EPON with IPD at room temperature and with a ratio of 100 g of EPON to 23.3 g of IPD. This mixture is placed into a Teflon mold with cylindrical cavities and cured in a vacuum oven at 30 mmHg. It is cured sequentially at 50 °C for 30 min and then at 100 °C for 1 hour. Samples were then stored in airtight sealed boxes to prevent environmental degradation.

2.2. Artificial weathering

In order to investigate the degradation of EPON under various conditions, a UV weathering tester was used (Q-Panel Q-lab Westlake, OH, USA). Fluorescent lamps (UVA- 340) with an irradiance level of 0.89 W/ $\rm m^2$ at 340 nm were used. The samples were subjected to two different exposure conditions: exposure to only UV radiation and cyclic exposure to UV radiation and moisture. For exposure to only UV radiation, specimens were exposed to UV irradiation at 60 °C for 0, 300 and 600 h and were named control, UV 300, and UV 600 respectively. For exposure to UV radiation and moisture, specimens were subjected to alternating cycles of 8 h of UV irradiation and 4 h of condensation at 60 °C without UV radiation. The specimens were also weathered for a total of 300 h and 600 h (including the radiation and condensation cycles) and were named UV 300-Cond and UV 600-Cond, respectively.

2.3. Fourier transform infrared spectroscopy

Attenuated total reflectance (ATR) spectra were obtained using a Fourier transform infrared spectrometer (ATR-FTIR, Bruker Lumos II) to detect changes in the chemical structures after weathering. Surfaces were tested with a $4\,\mathrm{cm}^{-1}$ resolution and 128 measurements were taken.

2.4. Scanning electron microscopy

A scanning electron microscope (Scios 2 Dual Beam FIB/SEM, Waltham, MA, USA) at an acceleration voltage of 5 kV was used for imaging to investigate the morphological changes due to UV only and UV with condensation exposure. The samples were sputter coated with a gold layer prior to imaging. Sample imaging for this paper was done at 1000x magnification.

2.5. SEM image analysis

Sample crack width and crevice area were analyzed using ImageJ software. For each exposure time, three sample were chosen and two micrographs were used for each sample analysis. SEM Images of different exposure samples are taken and then ImageJ software was used on the same area of each sample to analyze the width of the cracks and the size of the crevices.

2.6. Differential scanning calorimetry

The glass transition temperature of finely processed powder of EPON-IPD specimens weighing between 7 and 9 mg was determined using a differential scanning calorimeter (PerkinElmer DSC 4000, Houston, TX, USA). The powder was obtained by drilling near the surface then further crushing into a fine powder with a mortar and pestle. The specimens were placed in aluminum pans and heated from room temperature to 190 °C. The samples were heated from 30 °C to 190 °C at a rate of 10 °C/min and the glass transition temperatures were determined from this heating ramp.

2.7. Nanoindentation

The hardness, and elastic modulus of EPON-IPD were measured using a Nanoindenter (G-200 MTS, Agilent, and Santa Clara, CA, USA) with a Berkovich tip with a radius of 100 nm. EPON-IPD samples were placed on aluminum cylinders using crystal bond glue. Indentation at a depth of 10,000 nm and load of 0.5 mN were applied to the EPON-IPD samples. Individual indentation methods are used as the surface is significantly degraded so the indentations must be made carefully with operator attention.

2.8. Stress and shape recovery test

The shape memory properties of EPON-IPD were observed by first programming the SMPs by heating the material above the glass transition temperature ($T_{\rm g}$) to 170°C then compression to the desired strain (engineering strain of 20%) using an MTS Alliance Rt/100 Tensile compression force tester (MTS Systems Corporation, Eden Prairie, MN, USA) and finally then cooling back to room temperature. After samples ware cooled down to room temperature and unloaded, they were again placed back into the oven where stress and shape recovery tests were performed at 170 °C for 2 h.

3. Results and discussion

3.1. Thermal analysis

DSC measurements of glass transition temperatures for UV and combined UV and condensation weathered EPON-IPD are displayed in Table 1. An increase in $T_{\rm g}$ was observed in specimens aged by UV irradiation only. This was expected as an increase due to post-curing crosslinking is common in polymers in UV radiation over prolonged periods of time [18].

Crosslinking leads to a decrease in free volume which restricts the EPON-IPD polymer chain mobility and leads to the increase in glass transition temperature [19]. This result is consistent with a recent

Table 1Glass transition temperature of Control, UV300, UV600, UV300-Cond & UV600-Cond.

Sample	Cyclic UV Exposure (Hours)	Cyclic Moisture Exposure (Hours)	Glass transition temperature, T_g (°C)	Standard Deviation
Control	0	0	147.9 ℃	0.355
UV300	300	0	150.3 ℃	0.197
UV600	600	0	150.9 ℃	0.148
UV300-	200	100	147.5 °C	0.266
Cond				
UV600-	400	200	146.9 ℃	0.162
Cond				

review article on the durability of SMPs with aerospace conditions [20]. The opposite effect was noted in combined UV and condensation weathering. A slight decrease in glass transition was observed, with the highest decrease in the UV 600-Cond sample. When moisture is absorbed, characteristics of the specimens at different stages of exposure can drastically vary in hydrophilic and moderately hydrophilic materials such as epoxy polymers [21]. From Table 1, the change in $T_{\rm g}$ of about 1°C indicates the increase in the hydrophilic characteristic due to moisture absorption.

From Fig. 1, the glass transition temperature of the control sample is 147.9 °C and reached around 150.9 °C with increasing exposure to UV only. However, cyclic UV and moisture exposure caused the $T_{\rm g}$ to decrease to 146.9 °C. This is likely to be partially due to the breaking of crosslinks and scission of the polymer chains from hydrolysis. Introducing moisture into EPON-IPD also leads to water acting as a plasticizer, which spaces polymer chains apart from each other thus resulting in a lowered glass transition temperature from the increase in free volume [22]. The changes in $T_{\rm g}$ during the process correlated with changes in the mechanical properties of the SMP as seen in the following section and in literature [23].

3.2. Mechanical analysis

3.2.1. Nanoindentation: modulus and hardness

Photodegradation from UV and plasticization from moisture also affects the nanomechanical properties. Fig. 2(a) presents th results collected from the nanoindentation test for each sample of Control, UV300, UV600, UV300-Cond & UV600-Cond tested at 0.5mN load. At this load, the resulting penetration depth was approximately 10 μ m.

The modulus of a polymer reflects its ability to elastically store

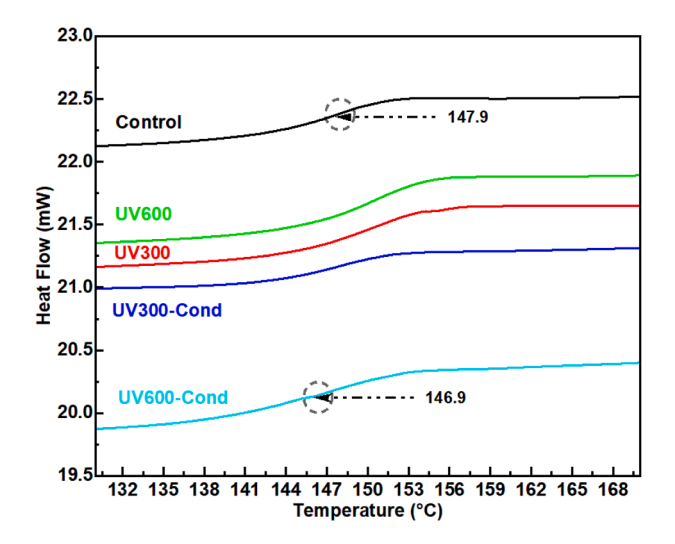


Fig. 1. Change of glass transition temperature in DSC thermograms of Control, UV300, UV600, UV300-Cond & UV600-Cond samples.

deformation energy, which is related to the degree of crosslinking. Furthermore, a rise in hardness indicates a loss of viscous dissipation or increased resistance to plastic deformation. The results clearly indicate that UV irradiation increase the elastic modulus and hardness of EPON-IPD SMPs which is consistent with other literature on the degradation of epoxy-based SMPs [20]. Nanoindentation results show that modulus increased 22% and hardness increased 33% after 600 h of UV radiation. This is attributed to the network and polymer chains breaking and reforming when exposed to UV light, which ultimately led to an increase in the crosslinking density of the SMP [24]. As evidenced by the occurrence of microcracks on nanoindentation marks during prolonged UV exposure, the nature of the indentation shifted from a ductile to brittle deformation [25] as seen in Fig. 2 (b,c,d).

UV irradiation combined with moisture resulted in physical changes in polymer with the modulus decreasing 15% and hardness decreasing 60% after 600 h of exposure. From Fig. 2 (e,f) it can be seen from the indentation images that the presence of moisture increases the plasticity of the polymer. It is evident that water can act as a plasticizer that increases molecular mobility and decreases modulus and hardness [26].

3.2.2. Compression and recovery test

To quantify the weathering effect on shape memory mechanisms outlined in this paper, fully constrained stress and strain recovery tests were performed on samples with compressive engineering strain of 20% programmed into the material. SMPs can release considerable stress if free recovery is not allowed [27]. Because of the conflicting requirements for recovery shape and recovery stress, most thermoset SMPs have good shape memory but poor stress memory [5,28]. SMPs with up to 7 MPa recovery stress are often regarded as having a high recovery stress output [29]. It is observed that ultraviolet radiation and moisture exposure have a strong effects on both shape recovery and stress recovery. Stress recovery is shown in Fig. 3 over time with the peak recovery stress shown in Table 2 and shape recovery is shown in the Table 3. From Fig. 3, it shows that the maximum 7.10 MPa stress recovery is obtained from the unweathered control sample and the minimum recovery stress is 5.75 MPa from UV600-cond sample.

UV radiation has been shown to reduce both the peak programming stress and peak recovery stress which is consistent with published research on other SMPs [30]. Because of the UV radiation, the peak recovery stress reduces to 6.84 MPa for UV 300 and 6.35 MPa for UV600. UV300-cond and UV600-cond exhibit a decrease in the peak stress recovery which is consistent with the work of Yang [31]. Degradation of the polymeric network of this high-enthalpy storage polymer reduces its ability to elastically store deformation energy, which results in less energy being available for recovery as indicated by the nearly proportional reduction in programming stress and the recovery stress. Cyclic exposure to moisture and UV radiation reduces the stress recovery of UV300-cond to 6.29 MPa and UV600-cond to 5.75 MPa which is 23.4% less than the control sample. The decrease in the recovery stress is due to the reduction of the elastic modulus. From Fig. 2, the nanoindentation test results also indicate that the elastic modulus is decreasing due to plasticization.

Two important criteria for describing shape memory behavior of SMPs, the shape fixity strain (R_f) and shape recovery strain (R_r) , can be determined from thermomechanical cycle. R_f quantifies the ability of the switching segment to fix the temporary deformation during the programming process whereas R_r measures the ability of the shape memory materials to recover their original shape [32]. The parameters are defined in Equations (1) and (2) below: The shape fixity strain is defined as the ratio of the retained strain after unloading $(\varepsilon_{\rm u})$ to the strain observed during loading $(\varepsilon_{\rm l})$ The shape recovery strain represents the difference between the strain after unloading and recovered strain $(\varepsilon_{\rm r})$ divided by the recovery strain $(\varepsilon_{\rm l})$ [33].

$$R_f = \frac{\epsilon_f}{\varepsilon}$$

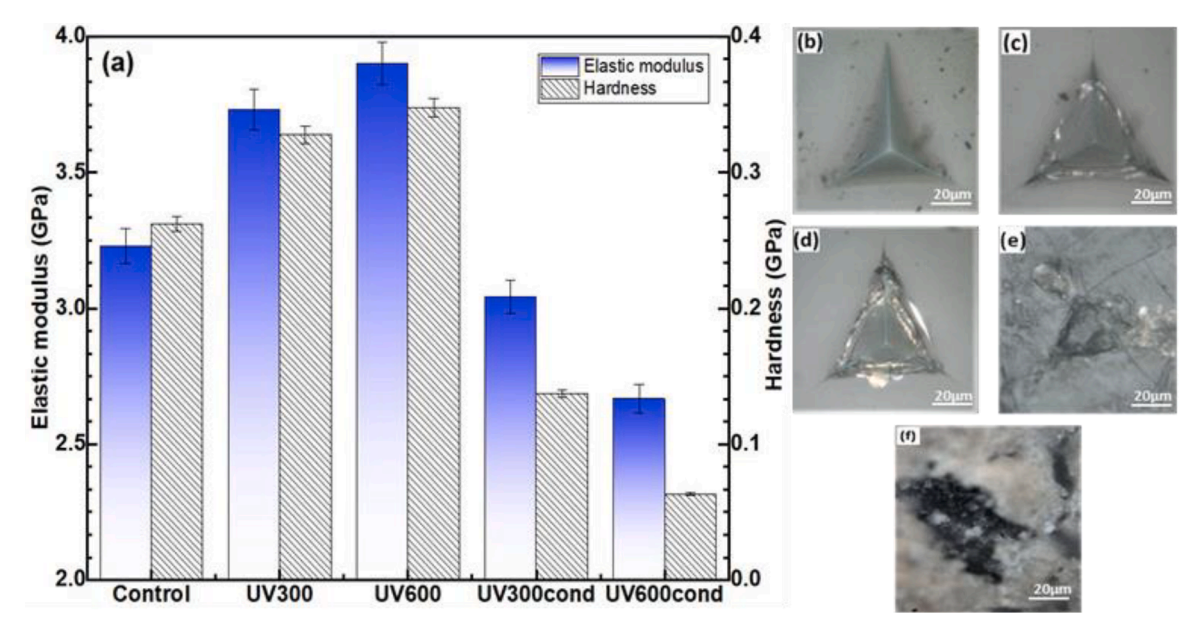


Fig. 2. (a) Nanoindentation result of elastic modulus and hardness at 0.5mN, and nanoindentation impressions of (b) Control, (c) UV300, (d) UV600, (e) UV300-Cond, and (f) UV600-Cond.

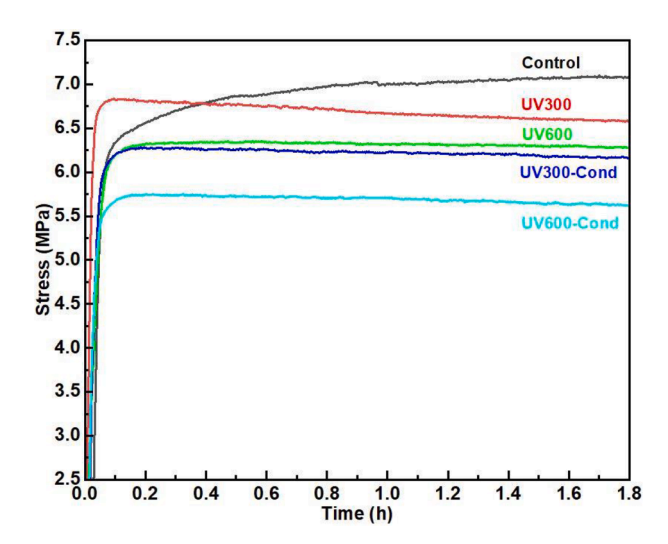


Fig. 3. Fully constrained stress recovery profile of Control, UV300, UV600, UV300-Cond & UV600-Cond (Recovered at 170 $^{\circ}$ C for 2 h).

Table 2 Stress-recovery results of compression programmed TSMPs.

Sample	Peak Programming Stress (MPa)	Peak Recovery Stress (MPa)	Percentage of Recovery Stress (%)
Control	8.75	7.10	81.1
UV300	8.40	6.84	81.4
UV600	7.78	6.35	81.7
UV300-	7.75	6.29	81.1
Cond			
UV600- Cond	7.44	5.75	77.4

$$R_r = \frac{\varepsilon_u - \varepsilon_r}{\varepsilon_r}$$

 R_f quantifies the ability of the switching segment to fix/hold the temporary compressed length ε_l when the compression was removed. In most SMPs, the sample will immediately expand from ε_u to a new length

 ε_{l} after the stress was removed. 100% shape fixity is when ε_{u} is equal to ε_{l} . A key characteristic of SMPs is their ability to restore their original shape after being heated above the glass transition temperature [31]. The high modulus below T_{g} and great rubber elasticity above T_{g} often result in outstanding shape fixity and recovery [34]. From Table 3, the results show that R_{f} is more than 90% for all the samples while every sample recovers over 95% of its original shape after heating over T_{g} . This high level of shape recovery indicates that the degradation is not so severe as to significantly enable plastic deformation on a molecular level that would allow for stress relaxation which would significantly reduce shape recovery [35]. In summary, the water and UV radiation significantly lower the recovery stress; however, they have little effect on shape recovery.

3.3. Chemical analysis

FTIR tests were run on the EPON-IPD samples to determine the effect of UV radiation and moisture condensation on thermal degradation and photo-oxidation. The characteristic bands of mixes were identified from the spectra at various wavenumbers and presented in Fig. 4.

Photo-oxidation can result in the generation of alkyl radicals, which can interact with polymer molecules to form hydro-peroxides through chain scission and other degrading mechanisms [35]. There were no notable changes in the core regions of the specimens before and after UV irradiation/combined irradiation and condensation as shown in Fig 4.

Table 3 Initial length, programmed length, post-recovery length and fixity and recovery strain of UV300, UV300, UV300-cond and UV600-cond (at 20% compressive strain).

Sample	Initial length, (mm)	Programmed length, (mm)	Post- Recovery, (mm)	Shape Fixity ratio (R _f)%	Shape Recovery ratio (<i>R_r</i>)%
Control	15.6	12.7	15.5	92.8	97.0
UV300	16.6	13.5	16.5	93.0	96.4
UV600	17.0	13.9	16.9	94.1	95.6
UV300-	15.6	12.8	15.5	90.6	97.4
cond					
UV600-	15.6	12.8	15.5	91.8	97.2
cond					

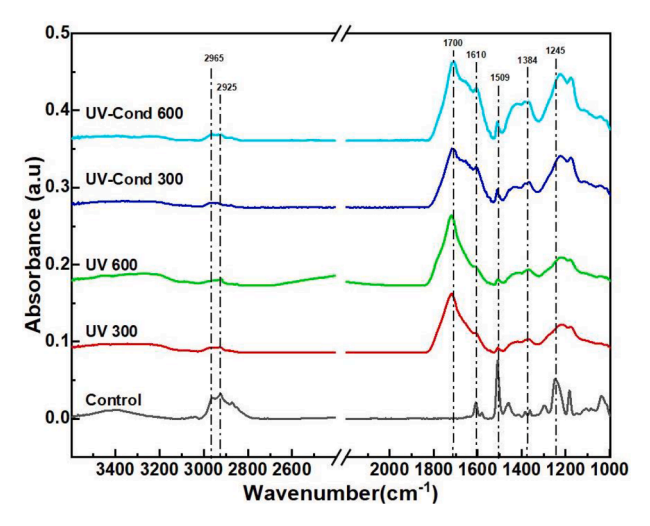


Fig. 4. FTIR spectra of Control, UV300, UV600, UV300-Cond & UV600-Cond samples.

However, the group of bands corresponding to the C—H stretching in the methylene group (between 2925 and 2965 cm $^{-1}$) on the control sample surface has diminished in all of the weathered samples. Further, the bands around $1700\ cm^{-1}$ and $1750\ cm^{-1}$ that are due to the stretching vibration of C = O in the ester/carboxylic acid/aldehydes were observed after UV irradiation as sharp peaks and broad humps in combined weathering of the samples. ^{35}The group of bands corresponding to the

-C=O vibration in the amide group at $1610~cm^{-1}$ is observed as sharp peaks in the control and UV samples. 35 The peaks appeared as broader humps in the weathered samples due to the formation of photodegradation products such as esters and carboxylic acids. The band at wavenumber $1509~cm^{-1}$ is the characteristic band for the benzene ring stretching of C=C, commonly found in DGEBA epoxy systems [35]. It is observed as a sharp peak in the pristine control and UV sample but is seen as a broad shoulder on the surfaces of weathered samples.

The development of a sharp peak due to the C=O symmetric stretching vibration of the carbonyl group was observed at $1716~\rm cm^{-1}$ in all degraded samples as shown in Fig. 5; however, the appearance of this peak was different for the samples degraded in both UV irradiation and condensation. For UV300-Cond and UV600-Cond samples, the peak appears as a broad node after the sharp peak at $1716~\rm cm^{-1}$. This is followed by a weak peak representing aromatic C=C stretching at $1610~\rm cm^{-1}$. The strong peak at $1509~\rm cm^{-1}$ is the aromatic stretching of DGEBA epoxy; it may also represent N–H deformation of cycloaliphatic amine

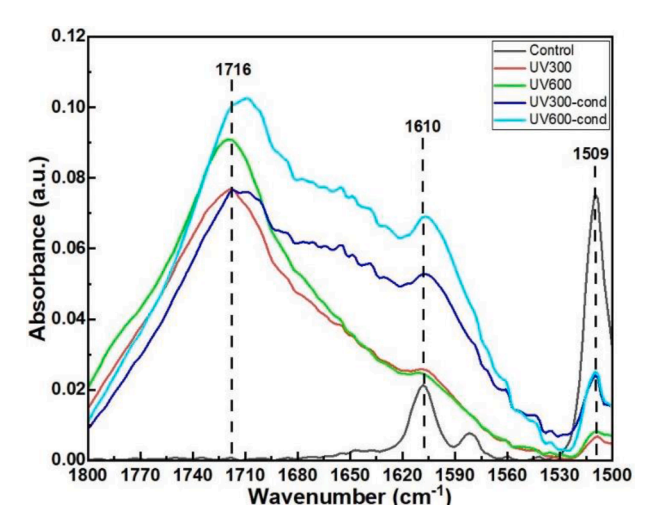


Fig. 5. FTIR spectra for carbonyl regions in TSMP system.

curing agent and N–H deformation of the polyamine cross-linker, respectively [36]. The reduction of both these peaks indicated the absorbance of atmospheric oxygen and suggested an increase in the crosslinking of the epoxy, particularly in the samples degraded by UV irradiation only [37]. This increased crosslinking leads to brittleness and can result in microcrack formation which can be corroborated with SEM findings.

It is observed that although the 1509 cm $^{-1}$ peak diminishes in all degraded samples, the presence of water aggravated the degradation for that peak [37]. Epoxies, being amorphous and having photo-labile groups, are highly susceptible to photo-oxidation. Moisture and small fluid molecules can easily penetrate within the amorphous chains, thereby increasing free volume in the system. The increased free volume will facilitate the diffusion of OH- and H+ ions and free radicals, thereby facilitating photo-degradation [38].

The combined effect of UV and moisture can be deleterious to the epoxies as the smaller degraded oligomers and monomers offer reduced resistance to photo-oxidation as compared to the unweathered epoxy. Further, as water molecules leach away soluble monomers and oligomers, the fresh layer underneath will be further exposed to degradation [37,39].

The presence of methyl groups of the isopropylidene bridge as indicated by a sharp peak with a wavelength of $1384~\rm cm^{-1}$ diminished in all degraded samples and turned into a broad node. However, the absorbance of this node was much higher in combined degradation. Moisture and UV cooperatively act to form hydro-peroxides and abstract hydrogen atoms to further exacerbate degradation in the combined weather cycle. A reduction with a slight shift towards $1240~\rm cm^{-1}$ around the peak at $1245~\rm cm^{-1}$ was also observed and was attributed to C–N asymmetric stretching vibrations due to amide formation. This observation indicates the occurrence of chain scission reactions as reported by other researchers [40-42].

3.4. Morphological analysis

A distinct change in color was apparent in all specimens exposed to simulated UV irradiation and/or moisture. From Fig. 6, yellowing was observed in the surface of the specimens. A gradual increase in color change was noted with increase in exposure duration. This observation is consistent with literature which attributes the color change to the formation of carbonyl groups due to photo-oxidation [8].

A scanning electron microscope was used to investigate the effect of degradation on the morphology of the specimens including crack formation. Fig.7 illustrated that the control specimen had no cracks apart from minor surface defects from sample preparation. While both UV and UV-Cond sample images exhibited degradation, significantly higher degradation was observed in the UV-Cond samples that underwent combined UV and condensation weathering.

Crevices were observed in both the UV 300 and UV 600 samples. These micro cracks have been known to be caused by internal stresses arising from crosslinking [43]. The process of photo-degradation was accelerated by the expansion of microcracks, which exposed the underneath polymer layer. Chain scission due to thermal stress causes embrittlement of the polymer [43].

Similar to the UV-only samples, microcracks were observed in UV Condensation samples, but they were also accompanied by craters and valleys. The presence of water exacerbates the degradation of the surface morphology of the shape memory polymer causing the SMP to become opaque. The observed craters are due to absorbed water or volatile components rapidly evaporating from the surface [44,45]. From comparison with other degradation studies on epoxies, these craters may be the result of blistering and subsequent eruption, but no active blisters were observed in the SEM study [46,47]. From the samples exposed to combined weathering, the valleys with the greater area were observed in the UV 600-Cond sample. From Table 4, image analysis determined that the UV 600-Cond sample had larger micro-cracks and valley area











Fig. 6. Optical image of color changing of Control (a), UV300 (b), UV600 (c), UV300-Cond (d) & UV600-Cond (e) samples.

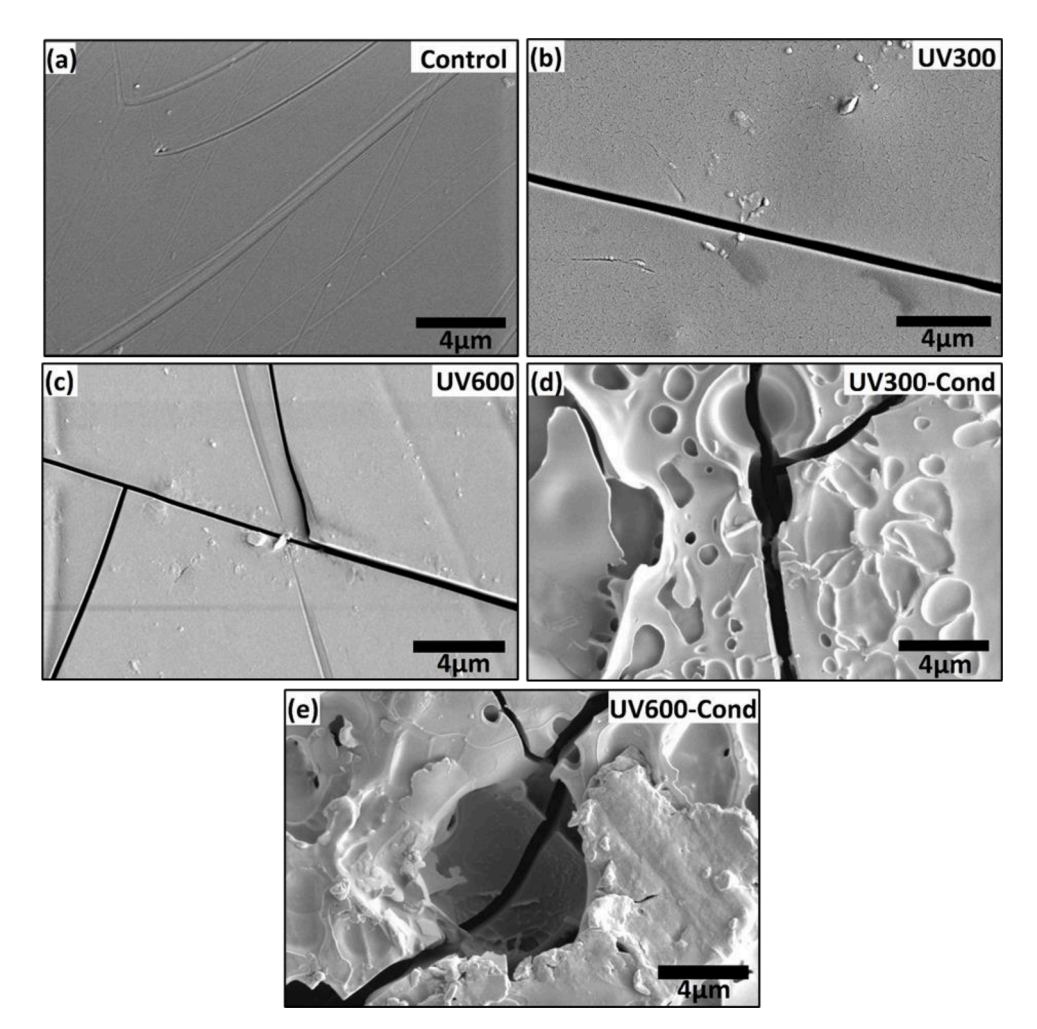


Fig. 7. SEM image of samples control (a), UV300 (b), UV600 (c), UV300-Cond (d) & UV600-Cond (e) with UV and moisture to represent surface morphology.

Table 4 Crack width and crevice area analysis of 0 h to 600 h samples with UV and moisture.

Sample	Average Crack Width, µm	Standard Deviation	Average Crevice Area, μm²	Standard Deviation
UV 300	0.349	0.079	_	_
UV 600	0.378	0.122	_	_
UV 300-	0.554	0.163	235.48	31.36
cond				
UV 600-	0.782	0.261	237.53	36.9
cond				

compared to both UV 600 and UV 300-Cond samples.

4. Conclusion

UV radiation and water absorption represent degradation mechanisms common to epoxy polymers. Exposure to UV light and condensation often had opposite effects. The T_g of the samples was increased when exposed only to UV light, but the T_g was reduced with combined exposure to UV radiation and condensation. UV radiation leads to an increase in the modulus and hardness, due to molecular recombination and crosslinking as determined by FTIR. Conversely, the presence of moisture reduces the modulus and hardness due to plasticization. The stress recovery was reduced in both the UV-only and cyclic condensation weathering conditions, indicating degradation of the chemical structure. SEM images indicated a loss of volatile products from the surfaces from

the samples exposed to cyclic condensation resulting in increased surface damage. From these results, it can be concluded that both the UV exposure and the cyclic condensation had significant, yet different effects on the investigated TSMPs, and the presence or absence of cyclic moisture exposure should be considered when modeling the performance of these TSMPs in their potential applications.

Declaration of Competing Interest

The authors declare that they have no known competing financial interests or personal relationships that could have appeared to influence the work reported in this paper.

Data availability

Data will be made available on request.

Acknowledgements

This work was primarily supported by the U.S. National Science Foundation under grant number OIA-1946231 and the Louisiana Board of Regents for the Louisiana Materials Design Alliance (LAMDA). This work was also supported by the Louisiana Board of Regents grant: LESQSF (2020–21)-ENH-DE-20. We thank Dr. Guoqiang Li (LSU) for providing the EPON-IPD samples.

References

- M.D. Hager, S. Bode, C. Weber, U.S. Schubert, Shape memory polymers: past, present and future developments, Prog. Polym. Sci. 49–50 (2015) 3–33.
- [2] T. Xie, Recent advances in polymer shape memory, Polymer (Guildf) 52 (2011) 4985–5000.
- [3] J. Li, Q. Duan, E. Zhang, J. Wang, Applications of shape memory polymers in kinetic buildings, in: Adv. Mater. Sci. Eng., 2018, 2018.
- [4] Y. Chen, Shape-memory polymeric artificial muscles: mechanisms, applications and challenges, Molecules 25 (2020) 1–27.
- [5] J. Fan, G. Li, High enthalpy storage thermoset network with giant stress and energy output in rubbery state, Nat. Commun. 9 (2018) 1–8, 2018 9:1.
- [6] T. Lu, E. Solis-Ramos, Y. Yi, M. Kumosa, UV degradation model for polymers and polymer matrix composites, Polym. Degrad. Stab. 154 (2018) 203–210.
- [7] W. Al Azzawi, J.A. Epaarachchi, J. Leng, Investigation of ultraviolet radiation effects on thermomechanical properties and shape memory behaviour of styrenebased shape memory polymers and its composite, Compos. Sci. Technol. 165 (2018) 266–273.
- [8] A.E. Krauklis, A.T. Echtermeyer, Mechanism of Yellowing: carbonyl Formation during Hygrothermal Aging in a Common Amine Epoxy, Polymers (Basel) 10 (2018) 1017, 2018, Vol. 10, Page 1017.
- [9] F. Xie, Effects of accelerated aging on thermal, mechanical and shape memory properties of cyanate-based shape memory polymer: I vacuum ultraviolet radiation, Polym. Degrad. Stab. C (2017) 91–97.
- [10] T. Pretsch, I. Jakob, W. Müller, Hydrolytic degradation and functional stability of a segmented shape memory poly(ester urethane), Polym. Degrad. Stab. 94 (2009) 61–73.
- [11] S. Shi, D. Shen, T. Xu, Programming effects on thermal decomposition of shape memory polymer-based composites, J. Therm. Anal. Calorim. 130 (2017) 1953–1960.
- [12] X. Zhang, Rapid, Localized, and Athermal Shape Memory Performance Triggered by Photoswitchable Glass Transition Temperature, ACS Appl. Mater. Interfaces 11 (2019) 46212–46218.
- [13] R.P. Singh, M. Khait, S.C. Zunjarrao, C.S. Korach, G. Pandey, Environmental degradation and durability of epoxy-clay nanocomposites, J. Nanomater. 2010 (2010).
- [14] Startsev, V.O. Effect of outdoor exposure on the moisture diffusion and mechanical properties of epoxy polymers. (2017) doi:10.1016/j.polymertesting.2017.12.007.
- [15] Y. Xia, Y. He, F. Zhang, Y. Liu, J. Leng, A Review of Shape Memory Polymers and Composites: mechanisms, Materials, and Applications, Adv. Mater. 33 (2021) 1–33
- [16] Niu, Y.F., Yang, Y., Li, T.Y. & Yao, J.W. Effects of UV irradiation and condensation on poly(ether-ether-ketone)/carbon fiber composites from nano- to macro-scale: 10.1177/0954008316689600 30, 230–238 (2017).
- [17] R. Mahmudzade, P. Nikaeen, W. Chirdon, A. Khattab, D. Depan, Photodegradation mechanisms and physico-chemical properties of EPON-IPD epoxy-based polymers, React. Funct. Polym. 178 (2022), 105351.
- [18] L. Hou, Y. Wu, B. Guo, D. Shan, Y. Zong, Degeneration and damage mechanism of epoxy-based shape memory polymer under 1 MeV electron irradiation, Mater. Lett. 222 (2018) 37–40.

- [19] H. Kim, M.W. Urban, Molecular level chain scission mechanisms of epoxy and urethane polymeric films exposed to UV/H2O. Multidimensional spectroscopic studies, Langmuir 16 (2000) 5382–5390.
- [20] S. Jayalath, Durability and long-term behaviour of shape memory polymers and composites for the space industry - A review of current status and future perspectives, Polym. Degrad. Stab. 211 (2023), 110297.
- [21] Startsev, O., Krotov, A. & Mashinskaya, G. Climatic Ageing Of Organic Fiber Reinforced Plastics: water Effect. 10.1080/00914039708031483 37, 161–171 (2006).
- [22] B. Yang, W.M. Huang, C. Li, J.H. Chor, Effects of moisture on the glass transition temperature of polyurethane shape memory polymer filled with nano-carbon powder, Eur. Polym. J. 41 (2005) 1123–1128.
- [23] Zhou, B., Liu, Y.J., Lan, X., Leng, J.S. & Yoon, S.H. A glass transition model for shape memory polymer and its composite. 10.1142/S0217979209060762 23, 1248–1253 (2012).
- [24] M. Bednarek, K. Borska, P. Kubisa, Crosslinking of Polylactide by High Energy Irradiation and Photo-Curing, Molecules 25 (2020).
- [25] A.G. Airale, M. Carello, A. Ferraris, L. Sisca, Moisture effect on mechanical properties of polymeric composite materials, AIP Conf. Proc. 1736 (2016), 020020.
- [26] L. Vertuccio, Behavior of epoxy composite resins in environments at high moisture content, J. Polym. Res. 20 (2013) 1–13, 2013 20:6.
- [27] A. Lendlein, S. Kelch, Shape-Memory Polymers, Encycloped. Polym. Sci. Tech. (2002), https://doi.org/10.1002/0471440264.PST336.
- [28] A. Li, J. Fan, G. Li, Recyclable thermoset shape memory polymers with high stress and energy output via facile UV-curing, J. Mater. Chem. A Mater. 6 (2018) 11479–11487
- [29] D. Santiago, A. Fabregat-Sanjuan, F. Ferrando, S. De La Flor, Recovery stress and work output in hyperbranched poly(ethyleneimine)-modified shape-memory epoxy polymers, J. Polym. Sci. B Polym. Phys. 54 (2016) 1002–1013.
- [30] W. al Azzawi, J.A. Epaarachchi, J. Leng, Investigation of ultraviolet radiation effects on thermomechanical properties and shape memory behaviour of styrenebased shape memory polymers and its composite, Compos. Sci. Technol. 165 (2018) 266–273.
- [31] B. Yang, W.M. Huang, C. Li, L. Li, Effects of moisture on the thermomechanical properties of a polyurethane shape memory polymer, Polymer (Guildf) 47 (2006) 1348–1356.
- [32] S.A. Abdullah, A. Jumahat, N.R. Abdullah, L. Frormann, Determination of Shape Fixity and Shape Recovery Rate of Carbon Nanotube-filled Shape Memory Polymer Nanocomposites, Procedia Eng. 41 (2012) 1641–1646.
- [33] J. Lee, S.K. Kang, Principles for Controlling the Shape Recovery and Degradation Behavior of Biodegradable Shape-Memory Polymers in Biomedical Applications, Micromachines (Basel) 12 (2021) 757.
- [34] Y. Liu, K. Gall, M.L. Dunn, A.R. Greenberg, J. Diani, Thermomechanics of shape memory polymers: uniaxial experiments and constitutive modeling, Int. J. Plast. 22 (2006) 279–313.
- [35] A. Cherdoud-Chihani, M. Mouzali, M.J.M. Abadie, Study of crosslinking acid copolymer/DGEBA systems by FTIR, J. Appl. Polym. Sci. 87 (2003) 2033–2051.
- [36] M.M. Khotbehsara, Effects of ultraviolet solar radiation on the properties of particulate-filled epoxy based polymer coating, Polym. Degrad. Stab. 181 (2020), 109352.
- [37] Kumar, B.G., Singh, R.P. & Nakamura, T. Degradation of Carbon Fiber-Reinforced Epoxy Composites by Ultraviolet Radiation and Condensation: 10.1177/0021 99802761675511 36, 2713–2733 (2016).
- [38] M.C. Celina, A.R. Dayile, A. Quintana, A perspective on the inherent oxidation sensitivity of epoxy materials, Polymer (Guildf) 54 (2013) 3290–3296.
- [39] G.F. Tjandraatmadja, L.S. Burn, M.C. Jollands, Evaluation of commercial polycarbonate optical properties after QUV-A radiation—The role of humidity in photodegradation, Polym. Degrad. Stab. 78 (2002) 435–448.
- [40] A. Tcherbi-Narteh, M. Hosur, E. Triggs, S. Jeelani, Thermal stability and degradation of diglycidyl ether of bisphenol A epoxy modified with different nanoclays exposed to UV radiation, Polym. Degrad. Stab. 98 (2013) 759–770.
- [41] P. Musto, M. Abbate, M. Pannico, G. Scarinzi, G. Ragosta, Improving the photo-oxidative stability of epoxy resins by use of functional POSS additives: a spectroscopic, mechanical and morphological study, Polymer (Guildf) 53 (2012) 5016–5036.
- [42] B. Mailhot, S. Morlat-Thérias, M. Ouahioune, J.L. Gardette, Study of the Degradation of an Epoxy/Amine Resin, 1, Macromol. Chem. Phys. 206 (2005) 575–584
- [43] R.S.C. Woo, Environmental degradation of epoxy-organoclay nanocomposites due to UV exposure. Part I: photo-degradation, Compos. Sci. Technol. 15–16 (2007) 3448–3456.
- [44] G.P. Mendis, I. Hua, J.P. Youngblood, J.A. Howarter, Enhanced dispersion of lignin in epoxy composites through hydration and mannich functionalization, J. Appl. Polym. Sci. 132 (2015).
- [45] S. Nikafshar, The Effects of UV Light on the Chemical and Mechanical Properties of a Transparent Epoxy-Diamine System in the Presence of an Organic UV Absorber, Materials (Basel) 10 (2017) 180, 2017, Vol. 10, Page 180.
- [46] S. Amrollahi, H. Yari, M. Rostami, Investigating the weathering performance of epoxy silicone nanocomposite coatings containing various loadings of Glycidoxypropyltrimethoxysilane-modified Zinc oxide nanoparticles, Prog. Org. Coat. 172 (2022), 107094.
- [47] J. Hu, X. Li, J. Gao, Q. Zhao, UV aging characterization of epoxy varnish coated steel upon exposure to artificial weathering environment, Mater. Des. 30 (2009) 1542–1547.